Journal of Chromatography A, 1426 (2015) 133–139

Contents lists available at ScienceDirect

Journal of Chromatography A

journal homepage: www.elsevier.com/locate/chroma

Characterization and quantification of histidine degradation in therapeutic protein formulations by size exclusion-hydrophilic interaction two dimensional-liquid chromatography with stable-isotope labeling mass spectrometry

Chunlei Wang*, Sike Chen, John A. Brailsford, Aaron P. Yamniuk, Adrienne A. Tymiak, Yingru Zhang

Research & Development, Bristol-Myers Squibb Company, P.O. Box 4000, Princeton, NJ, 08540, USA

ARTICLE INFO

Article history:
Received 10 September 2015
Received in revised form
17 November 2015
Accepted 19 November 2015
Available online 23 November 2015

Keywords:
Two-dimensional liquid chromatography
Stable-isotope labeling mass spectrometry
Quantification
Protein formulation
Histidine degradation

ABSTRACT

Two dimensional liquid chromatography (2D-LC) coupling size exclusion (SEC) and hydrophilic interaction chromatography (HILIC) is demonstrated as a useful tool to study polar excipients, such as histidine and its degradant, in protein formulation samples. The SEC-HILIC setup successfully removed interferences from complex sample matrices and enabled accurate mass measurement of the histidine degradation product, which was then determined to be *trans*-urocanic acid. Because the SEC effluent is a strong solvent for the second dimension HILIC, experimental parameters needed to be carefully chosen, i.e., small transferring loop, fast gradient at high flow rates for the second dimension gradient, in order to mitigate the solvent mismatch and to ensure good peak shapes for HILIC separations. In addition, the generation of *trans*-urocanic acid was quantified by single heart-cutting SEC-HILIC 2D-LC combined with stable-isotope labeling mass spectrometry. Compared with existing 2D quantification methods, the proposed approach is fast, insensitive to solvent mismatch between dimensions, and tolerant of small retention time shifts in the first dimension. Finally, the first dimension diode array detector was found to be a potential degradation source for photolabile analytes such as *trans*-urocanic acid.

1. Introduction

Protein therapeutics, especially monoclonal antibodies, constitute the most rapidly growing class of pharmaceutical drugs [1–3]. Indeed, 8 out of the 10 top selling drugs in 2013 are protein therapeutics [2], targeting autoimmune diseases, diabetes and cancers. Hundreds of protein drug candidates are currently under clinical development covering diseases in autoimmunity, inflammation, cancer, infection, ophthalmology, and other indications [2–4]. In general, protein drugs are highly specific for disease targets, offer unique efficacy with less side effects, and are better tolerated than small molecule drugs [3–5]. On the other hand, proteins are complex molecules that are susceptible to chemical and physical degradations such as deamidation, oxidation, hydrolysis, aggregation, conformational changes, surface adsorption, and precipitation [3,6].

These protein degradations can be minimized by selecting optimal excipients during formulation development [6–8]. Appropriate excipients have shown to stabilize protein drug molecules and maintain the drug's potency under stressed conditions during processing, storage, and distribution. In addition to promoting stability, excipients are also used in protein formulations to control drug delivery, improve solubility, preserve product sterility, and provide tonicity [7,8]. Most commonly used excipients include buffering agents controlling solution pH, salts adjusting solution osmolality, carbohydrates as stabilization agents, and surfactants as solubilization agents [7,8].

While excipients are used to stabilize protein therapeutics, there is a growing concern that the impurity profiles and degradation products of excipients can potentially impact protein stability [8–13]. For example, Wasylaschuk et al. reported substantial concentrations of hydroperoxides in some common excipients including polysorbate 80 and polyethylene glycol 400 [9]. Valliere-Douglass et al. showed that photochemical degradation products from citrate formulation buffer caused carbonylation on the N-termini and lysine side chains of recombinant monoclonal antibodies [10]. Subramanian et al. observed a significant loss of

* Corresponding author. Tel.: +1 609 252 5950.
E-mail address: chunlei.wang@bms.com (C. Wang).

http://dx.doi.org/10.1016/j.chroma.2015.11.065
0021-9673/

potency of a monoclonal antibody and attributed it to an oxidation product from histidine formulation buffer [13].

Li et al. recently reported different degradation rates of polysorbate 20 esters depending on the presence of antibodies, and demonstrated the importance of studying excipients stability in protein formulations for drug formulation development [14]. However, there are very few reported studies of excipient degradation in formulated protein therapeutics [14]. This is likely due to the challenges originating from the incompatibility or interference of protein drug molecules with many analytical techniques that are suitable for small molecule excipients. Most studies bypassed the complex protein formulation matrices, and studied buffer degradation by itself or with single amino acids and short chain oligopeptides to mimic therapeutic proteins that have much higher molecular weight [10–12].

Multidimensional chromatography, employing more than one separation mechanism [15–22], is particularly well suited for the study of excipient degradation in the complex matrices of proteins and excipients, both of which are often at high concentrations. The most common form of multidimensional chromatography is two-dimensional (2D) chromatography. In principle, protein drug molecules can be separated by the first dimension, and the excipients fraction can be obtained by heart-cutting and further analyzed using another suitable chromatographic mode. The sample transfer between the two dimensions can be achieved either offline or online. The offline method involves fraction collection from the first dimension, often times requiring fraction concentration, and then re-injection onto the second dimension. Alternatively, the online technique uses switching valves and sample loops to transfer the fractions from the first dimension (^{1}D) to the second dimension (^{2}D). The offline approach is widely adapted due to its simplicity in terms of instrumentation. However, with the advancement and commercialization of new 2D-LC instruments, the online approach is becoming the preferred option because it is a closed system avoiding sample loss, is faster and is more reproducible [17].

In the recent study of polysorbate 20 stability in monoclonal antibody formulations [14], Li et al. used a mixed mode online SPE cartridge in the first dimension to trap the hydrophobic polymer while removing proteins and hydrophilic excipients. The polysorbate 20 was then eluted with strong organic solvent, stored in an online sample loop, and subjected to the reversed-phase analysis on ^{2}D. An ion-exchange column was also tested to provide the first dimension separation, where all the excipients were eluted at the void volume and transferred online for ^{2}D analysis. With the 2D-LC separation to removing matrix effects, the heterogeneity and stability of polysorbate 20 molecular species present in monoclonal antibody formulations were successfully characterized.

In this study, we present an online heart-cutting 2D-LC method that couples size exclusion chromatography (SEC) with hydrophilic interaction chromatography (HILIC), providing a second dimension that is more suitable to study the hydrophilic excipients that are commonly used for protein formulations. A growing histidine degradation product in protein stability samples was successfully characterized by the SEC-HILIC 2D-LC method. The effects of experimental parameters on ^{2}D peak shapes are evaluated. In addition, quantification by stable-isotope dilution mass spectrometry was demonstrated for the heart-cutting 2D analysis. Finally, potential effects of ^{1}D diode array detector (DAD) on photolabile compounds are discussed.

2. Material and methods

2.1. Material

Protein formulation excipients including histidine, sorbitol, sucrose and sodium chloride were purchased from JT Baker (Center Valley, PA, USA). [$^{13}C_6$,$^{15}N_3$]-L-histidine, Chromasolv gradient grade acetonitrile, formic acid and all chemical reagents for synthesis of stable labeled urocanic acid were obtained from Sigma-Aldrich (St. Louis, MO, USA). High purity deionized water was supplied by the Barnstead Nanopure system from Thermo Scientific (Waltham, MA, USA). The protein stability sample was generated in house. The samples used in impurity identification part are adnectin proteins [23] formulated in 50 mM histidine, 100 mM sodium chloride and 5% sorbitol at pH 6.5. The samples used in the rest of the study are pegylated proteins formulated in 20 mM histidine and 250 mM sucrose at pH 6.5.

2.2. Preparation of stable-labeled trans-urocanic acid

[$^{13}C_6$,$^{15}N_2$]-*trans*-urocanic acid was prepared following a literature procedure [24]. Specifically, [$^{13}C_6$,$^{15}N_3$]-L-histidine (0.200 g, 1.219 mmol) was suspended in 0.5 mL of anhydrous MeOH and cooled in an ice bath. Methyl iodide (0.200 mL, 3.19 mmol) in 0.2 mL of MeOH, KOH (0.179 g, 3.19 mmol) in 0.6 mL of MeOH were added subsequently into the histidine solution by syringe and the solids dissolved. The mixture was stirred for 1 h at 0 °C and then warmed to room temperature (rt). The pH of the mixture was found to be neutral. A second portion of methyl iodide (0.100 mL, 1.597 mmol) in 0.1 mL of MeOH, and KOH (0.090 g, 1.597 mmol) in 0.3 mL of MeOH were added. After stirring for 30 min at rt, the pH of the solution was neutral and the mixture was concentrated on the rotovap to remove MeOH and dried on high vacuum to yield an off-white solid. The desired intermediate was observed by LC/MS (ESI$^+$ m/z 207) along with a side product resulting from *N*-methylation of the imidazole ring (ESI$^+$ m/z 221). The quaternary amine intermediate was suspended in 1.3 mL of 30% NaOH (aq) and heated at 110 °C for 18 h then cooled to rt. Upon heating the solids dissolved. The mixture was adjusted to pH 6 using 6N HCl, and then concentrated on the rotovap to an off-white solid. The solid material was extracted with EtOH and concentrated to yield a white solid product. The crude product was purified by prep HPLC on a ZIC-HILIC, 150 × 21.2 mm, 5 μm prep column (EMD Millipore, Billerica, MA, USA) to yield [$^{13}C_6$,$^{15}N_2$]-*trans*-urocanic acid as a white solid (86 mg, 48% yield, >99% HPLC purity). ^{1}H NMR (400 MHz, DMSO-d_6) δ 12.63 (br s, 1H), 8.87 (dm, $^1J_{CH}$ = 221 Hz, 1H), 7.93 (dm, $^1J_{CH}$ = 220 Hz, 1H), 7.49 (dm, $^1J_{CH}$ = 156 Hz, 1H), 6.54 (dm, $^1J_{CH}$ = 162 Hz, 1H); MS ESI$^+$ [M + H]$^+$ = 147.12, mass isotopic distribution m/z 147.12 (95.52%), 146.12 (4.28%).

2.3. 2D LC setup

The 2D-LC was built from an Agilent (Santa Clara, CA, USA) 1290 LC system. Three different valve setups were employed in the study (Fig. 1). The first setup (Fig. 1A) was home built and was used for the impurity identification, which employed a 2-position 6 port valve and a 10 μL transferring loop that were housed in the G1316 C column oven. Agilent 1100 binary pump G1312A and DAD detector G1315B were used for ^{1}D. The MassHunter software v4.0 from Agilent was used to control the instrument, collect and process the data for the first setup. The second and third setups were commercial solutions delivered by Agilent and were used for ^{2}D peak shape and quantification studies. These two setups used the same Agilent G1170A valve, but plumbed differently for cocurrent (Fig. 1B) and countercurrent (Fig. 1C) heart-cutting experiments. Agilent 1290 quarternary pump G4204A and 1260 DAD detector G4214B with G4212-60008 flow cell (10 mm, 1 μL) were used for ^{1}D separation. All three setups shared the same sample injector and ^{2}D modules, i.e., G4226A autosampler with G1330B temperature controlling unit, 1290 binary pump G4220A, 1290 G4212A DAD detector with G4212-60007 flow cell (60 mm, 4 μL), and 6224

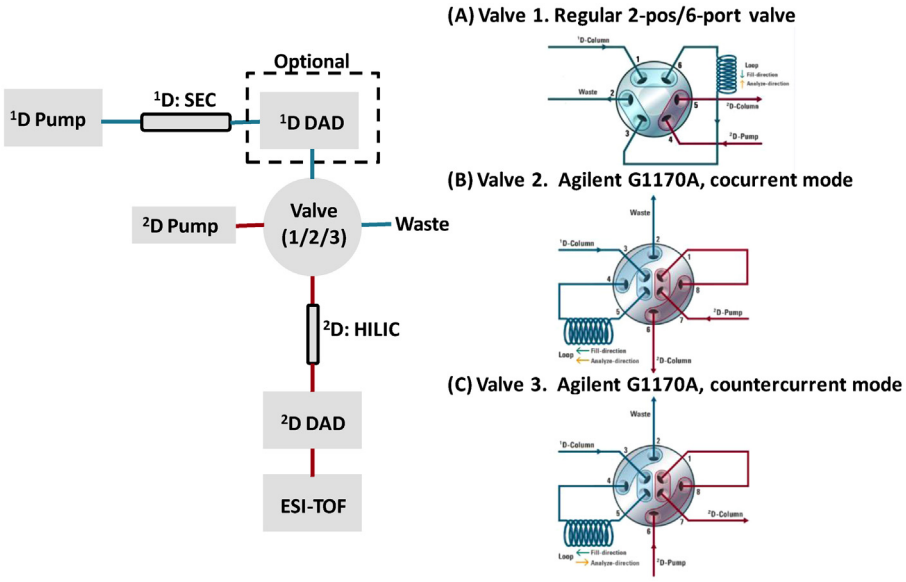

Fig. 1. Schematic of 2D-LC systems, with the ^{1}D DAD as optional. Three different valve setups are used: (A) traditional 2-pos/6-port valve; (B) Agilent G1770A valve with cocurrent option; (C) Agilent G1770A valve with countercurrent option. All valves are in the filling position. The ^{1}D and ^{2}D flow are shown in blue and red, respectively.

TOF mass spectrometer. The second and third setups were operated using OpenLAB CDS vC.01.07 software, and the MS data were collected and processed by MassHunter software v4.0.

Two brands of SEC columns were used for ^{1}D. The impurity identification experiments were conducted on a Sepax (Newark, DE, USA) Zenix-C 300 column, 300 × 4.6 mm, using water/acetonitrile/formic acid/trifluoroacetic acid 60/40/0.2/0.01 as mobile phase solvent running at 0.35 mL/min. Another custom made Zenix-C 300 column, 150 × 1.0 mm, was used in the photodegradation ^{1}D flow cell study. Waters BEH200 SEC, 150 × 4.6 mm, 1.7 μm column (Milford, MA, USA), was used for the rest of the studies running water/acetonitrile/formic acid 80/20/0.2. Instead of using high concentration of inorganic salts that are typically used for SEC, we chose 20% acetonitrile with formic acid to avoid potential precipitation in the ^{2}D column and to prolong the lifetime of the 2D transferring valve. Using the salt-free aqueous organic mobile phase, the size-based separation between proteins and small molecular formulation excipients were also preserved. The second dimension hydrophilic interaction chromatography (HILIC) was performed on a phosphorylcholine-based zwitterionic column, i.e., ZIC-HILIC, 150 × 4.6 mm, 5 μm column (EMD Millipore, Billerica, MA, USA). The mobile phase A was acetonitrile with 0.1% formic acid, and B was water with 0.1% formic acid. The gradient was 10–50% B in 10 min with 3 min re-equilibration time at a flow rate of 0.7 mL/min unless otherwise specified. Both columns were kept at the room temperature of 22 °C.

The accurate mass and quantification was measured by the TOF-MS with the following instrument settings: the capillary voltage of 3.5 kV, the nebulizer gas at 40 psi, and drying gas at 13 L/min with gas temperature of 350 °C. The fragment, skimmer, and OCT 1 RF Vpp voltage were 130 V, 65 V, and 750 V, respectively. The acquisition rate for the MS scan was 1 spectra/s.

3. Results and discussion

3.1. Histidine degradation in protein stability samples

There have been several reports on degradation of histidine when used as a formulation agent for protein therapeutics [12,13]. During one of our recent stress stability studies of protein

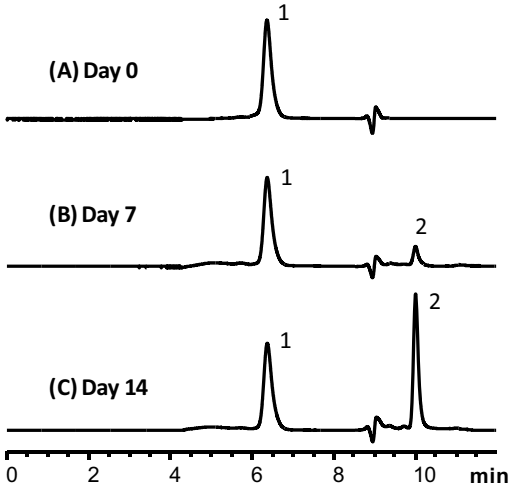

Fig. 2. SEC chromatograms of an adnectin protein, formulated in pH 6.5 histidine buffer, at different time points of a stability study: (A) beginning of the study; (B) 7 days; (C) 14 days. Peak 1 is the protein, and peak 2 is the growing unknown peak.

therapeutics, we also observed increasing levels of a UV absorbing peak at the total permeation volume under SEC conditions, as shown in Fig. 2. In order to identify the growing unknown peak, direct coupling of SEC to a MS detector was attempted by using volatile buffers for SEC separations. Unfortunately, the unknown peak coeluted with formulation excipients, containing 50 mM histidine and 5% sorbitol, which caused severe ion suppression and made the mass identification of the unknown species unsuccessful. In the previous report, we used the offline 2D approach to identify the unknown peak as *trans*-urocanic acid (*t*-UA) [25], a deamination product from histidine degradation. As pointed out by one reviewer, sample preparation by ultrafiltration could potentially replace the ^{1}D SEC separation. In our case, however, it was very challenging to recover any filtrate for quantification due to the small sample volume (~20 μL) in our protein stability study. In addition, a more simplified workflow with minimal sample preparation was also preferred. In the current work, we demonstrate how online 2D-LC, combining SEC with HILIC, can be used for qualitative

and quantitative analysis of such highly polar excipients in protein formulation samples.

3.2. Impurity identification by online 2D-LC coupled to high resolution MS

With the online heart-cutting 2D approach, the unknown peak as observed by SEC can be trapped by a sampling loop, and directly transferred to the ^{2}D HILIC column by valve switching. Fig. 1 shows the schematic diagram of the heart-cutting 2D-LC system used. Using our homemade 2D system assembled several years ago (Fig. 1A), an extra scouting injection was needed to obtain the SEC elution time of the targeted peak, which was then used to set valve switching time for heart-cutting 2D analysis in the subsequent injection. Nowadays, with the growing customer interests and the maturing hardware and software in 2D-LC, many vendors provide automated solutions that support peak detection based heart-cutting. As a result, a single injection is all that is it needs to remove the sample matrix, trap the peak on the fly, and analyze it in ^{2}D. As compared to the offline approach, the online 2D approach greatly reduces sample manipulation while it simplifies and automates the workflow.

Fig. 3 shows the heart-cutting SEC-HILIC analysis of the protein stability sample. Fig. 3A is the ^{1}D SEC UV chromatogram, where the peak at 11 min is the unknown peak eluting at the total SEC permeation volume, along with formulation excipients. Fig. 3B–E are UV, Total Ion (TIC) MS and Selected Ion (SIM) MS chromatograms of the ^{2}D HILIC separation. The only major peak at 21.5 min under UV 280 nm (Fig. 3B) was the unknown species. As shown in TIC (Fig. 3C), the unknown peak was well resolved from formulation excipients, thus free from ion suppressions. Sorbitol was eluted to the front of the unknown (Fig. 3D), and histidine did not elute until the gradient end. The mass spectrum of the unknown peak shared the same in source fragmentation ion as observed with histidine at *m/z* 94, which suggested that it was derived from histidine.

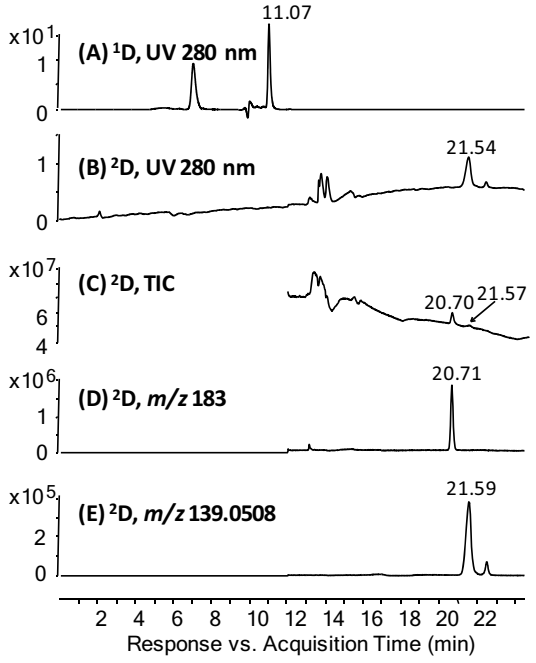

Fig. 3. SEC-HILIC analysis of the protein stability sample. (A) ^{1}D SEC chromatogram at UV 280 nm. (B–E) ^{2}D HILIC chromatograms: (B) UV 280 nm; (C) TIC; (D) EIC at *m/z* 183 for protonated sorbitol; (E) EIC at the identified accurate mass of the unknown. The unknown peak was separated from excipients, sorbitol and histidine, and was detected by MS free from ion suppression. ^{2}D gradient: 90-90-50%B (acetonitrile with 0.2% formic acid) at 0-11-26 min with 0.7 mL/min flow.

Based on the accurate mass, *m/z* 139.0508, the peak was tentatively assigned as the histidine deamination product urocanic acid, $C_6H_6N_2O_2$ with a 4 ppm error in accurate mass. With the first and most important piece of information obtained by 2D-LC/MS, additional experiments were carried out to confirm the unknown to be *t*-UA [25].

3.3. Peak shapes on ^{2}D HILIC separation

The negative impact of ^{1}D effluent on ^{2}D separation, or solvent incompatibility between two hyphenated separations, is one of the major challenges for 2D applications [26,27]. Different approaches have been employed to overcome solvent incompatibility between two dimensions, such as adding a trap-and-elute column in-between dimensions [28], diluting ^{1}D effluent with counter gradients or ^{2}D weak solvent [26,27], and introducing on-column focusing by manipulating temperatures [29]. In our application, the highly aqueous SEC mobile phase is a strong injection solvent for the ^{2}D HILIC separation, whose performance could potentially be compromised. Instead of introducing extra hardware, i.e., trap columns or dilution pumps, we focused on reducing the solvent incompatibility by optimizing ^{2}D chromatographic parameters.

To achieve better sensitivity for ^{2}D quantification, large loop size is usually preferred to transfer more fraction between two dimensions. Fig. 4A–C shows the effects of transferring loop size on ^{2}D peak shape. A broad blob was observed with a 500 μL loop. As expected, the peak became narrower and more symmetric as the injection volume and transferring loop size decreased. Agilent 2D valves provided two options to load ^{1}D fraction on ^{2}D, i.e., cocurrent and countercurrent modes. In the cocurrent mode, ^{1}D filling flow and ^{2}D depleting flow in the transferring loop follow the same direction. Fig. 4C and D compares the 2D peak shape obtained with the same sample plug size when 100 and 500 μL loops are used in the cocurrent mode. The retention time at the peak apex was identical in both cases. With the 500 μL loop, however, the peak was much wider and fronting shaped. It is probably due to the

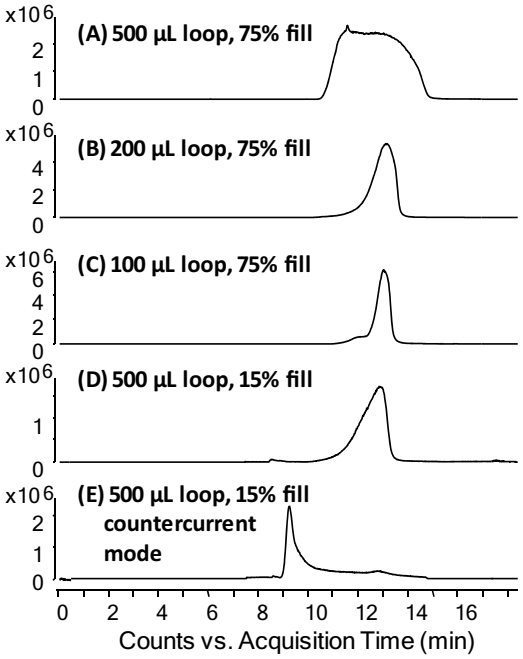

Fig. 4. Effects of loop size and valve configuration on ^{2}D HILIC peak shape of *t*-UA. (A, B, C), cocurrent mode, 75% fill volume in 500, 200, and 100 μL transferring loops, respectively. (D, E), 15% fill volume in a 500 μL transferring loop in cocurrent and countercurrent mode, respectively.

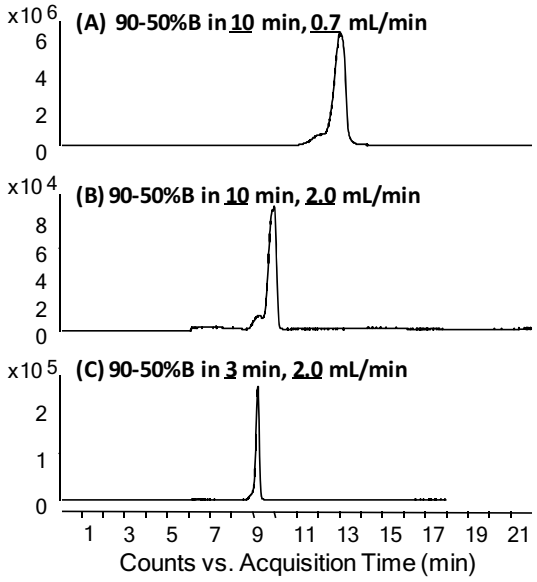

Fig. 5. Effects of ^{2}D HILIC gradient profile on *t*-UA peak shape using a 100 μL transferring loop in cocurrent mode. (A, B), 90–50% organic in 10 min with 0.7 and 2.0 mL/min flow rates, respectively; (C), 90–50% organic in 3 min at 2.0 mL/min flow. The ^{2}D started at 6.7 min.

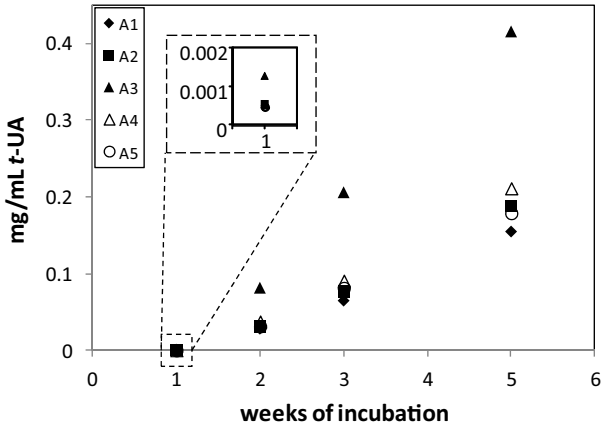

Fig. 6. The generation of *t*-UA in five protein formulation samples (A1–A5) during a 5 weeks' stability study. The temperature was held at 25 °C for 1 week, and then elevated to 40 °C for rest of the study. No *t*-UA was observed at the beginning of the study. The *t*-UA content at 1 week time point was shown in the insert at enlarged scale.

disruption of the column bed by the larger plug of strong solvent that was loaded to ^{2}D to the front of sample plug, which then leads to reduced retention when the analyte diffuses from the sample plug to the front strong solvent. When filling 15% of a 500 μL in the countercurrent mode (Fig. 4E), two peaks were observed, i.e., one major tailing peak with much reduced retention and one small hump at the expected retention time. It is likely that the large plug of strong solvent served as the actual mobile phase to elute most of the analyte out at reduced retention. Any residual sample that was able to diffuse out of the plug of strong solvent would still register a normal retention time. In short, the cocurrent and countercurrent options can produce dramatically different peak profiles, but keeping a small loop size is vital to reduce the solvent mismatch between two dimensions.

In addition to the loop size, gradient profiles can also affect peak shapes of the ^{2}D HILIC separation. For example, with the same loop size of 100 μL, the peak shape improved dramatically with higher flow rates, and faster gradient times, as shown in Fig. 5. It is worth noting that while a faster gradient time reduces retention, higher flow rate actually, on the other hand, leads to larger retention factor and better resolution as long as the high flow rate does not lead to a dramatic increase in plate heights. In our case, a symmetric Gaussian peak can be obtained for the ^{2}D HILIC separation on a 150 × 4.6 mm column using a gradient of 90–50% organic over 3 min time at 2 mL/min flow rate (Fig. 5C). Under these conditions, the separation of *t*-UA from other formulation excipients was still maintained. The injection volume of 100 μL for ^{2}D was approximately 5% of the column volume, and is 5 times the volume recommended by the manufacturer. Finally, the tolerance of peak shapes on injecting in strong solvents also depends on retention times. Species with longer retention time are less susceptible to peak distortion by strong solvent injections.

3.4. Quantification

Online 2D-LC, achieved with fully automated valve systems tended to produce more reproducible quantification results than obtained using an offline approach. Quantification can be obtained using comprehensive, or selected comprehensive 2D where only the retention time range of targeted peaks are fractioned and transferred for ^{2}D analysis [30]. The peak area of multiple ^{2}D injections are then summed for calculations. However, comprehensive and selected comprehensive 2D demand more data processing and require more time to acquire data, especially when the ^{2}D run time is long. Heart-cutting 2D has also been used for quantification. The whole peak is usually transferred to ^{2}D as a single slice [31,32], sometimes with the help of trap columns [33]. The quantification based on a ^{2}D chromatogram is not much different from traditional one dimensional analysis. Quantitative analysis by cutting just part of ^{1}D peak at fixed time windows has also been evaluated [30]. Potential peak shifts in ^{1}D could compromise the method reproducibility and robustness.

In our study, the deleterious effects of solvent mismatch on ^{2}D HILIC peak shapes preclude whole ^{1}D SEC peak transfer. Additional modifications to the existing 2D setup, such as diluting the ^{1}D eluent prior to heart-cutting by an additional pump [26,34], could potentially solve the solvent mismatch problem. Fortunately, the concentration of *t*-UA in our samples was high enough to allow the ^{2}D detection even without transferring the whole ^{1}D peak. Hence, we choose to transfer only parts of the peak to minimize the impact of solvent mismatch. To overcome the reproducibility issue associated with partial peak transfer, we employ stable-isotope dilution mass spectrometry for accurate quantification. Good linearity between the peak area ratios (analyte/internal standard) and the concentration of the calibration standards were observed in the range from 0.1 μg/mL to 1000 μg/mL. The determination coefficient is 0.9999 for the $1/x$ weighted linear fit in the calibration range. The %RSD (n = 5) at 0.1 μg/mL (LOQ) and 0.5 μg/mL standards (the level of lowest sample concentration) is 9% and 4%, respectively. The spike recovery of 1 μg/mL standard is 102% ± 2% (n = 3).

Five protein stability samples (A1–A5) were incubated for 25 °C for 1 week, and then held at 40 °C for another 4 weeks. Samples at each time point were frozen at −80 °C until being analyzed together for *t*-UA generation. The *t*-UA was observed in all samples except for time zero (Fig. 6). On average, only 0.7 μg/mL *t*-UA was observed after incubating 25 °C for 1 week. At 40 °C, the histidine degradation to *t*-UA was approximately 90 times faster as compared to that at 25 °C. By the end of the study, formulation sample of A3 contained 0.46 mg/mL *t*-UA, i.e., corresponding to 17% histidine deamination degradation. The rate of production of *t*-UA in formulation samples of the other four proteins is roughly half of that observed for A3. Since these proteins were prepared from the same stock buffer solution and were incubated under the same stress

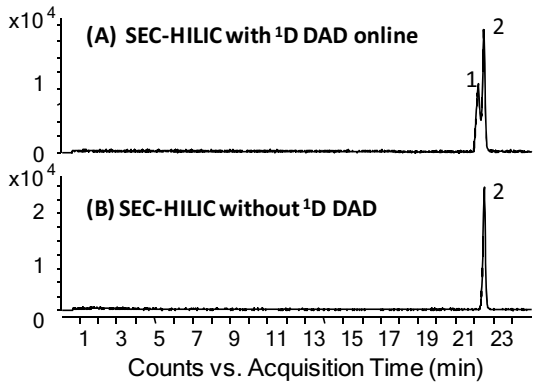

Fig. 7. Comparing ^{2}D HILIC chromatograms with (A) and without (B) active ^{1}D DAD. Peak 1 is *c*-UA; peak 2 *t*-UA. ^{1}D, 100 μL/min of water/acetonitrile/formic acid 80/20/0.2 on Waters BEH200 SEC column. The transferring loop was 80 μL with 75% fill volume. ^{2}D started at 20.13 min running a gradient of 90–50% organic in 3 min at 2 mL/min.

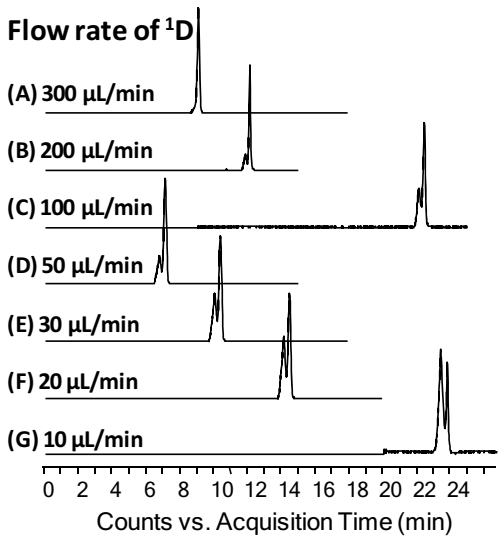

Fig. 8. Effects of reducing ^{1}D flow rates on the generation of *c*-UA (the front peak) on ^{2}D chromatograms: (A–G), 300, 200, 100, 50, 30, 20, 10 μL/min. (A–C) were run on a 150 × 4.6 mm Water BEH200 SEC column; (D–G) on a custom made 100 × 2.1 mm Sepax Zenix-C 300 column. Loop and ^{2}D parameters are the same as that for Fig. 7. ^{2}D starting times varied according to the ^{1}D column and flow rates.

conditions, the observed different histidine deamination kinetics suggests that proteins may play a role in such degradation.

These five proteins were engineered to eliminate the deamidation risks and to reduce the acidic variants as measured by imaged capillary isoelectric focusing (icIEF). Interestingly, however, all except A3 showed dramatically reduced acidic variants during icIEF analysis. The coincidence between accelerated histidine deamination and the high levels of protein acidic variants in A3 warrants further investigation to evaluate whether there is a causal relationship between the two observations.

3.5. ^{1}D DAD detector, to use or not to use

State-of-art 2D-LC systems all come with multiple DAD detectors, with each for a different dimension. In the heart-cutting mode, ^{1}D detector is required to either pre-determine the timing of valve switching or register signals and trigger the automated valve switching during the analysis. In the comprehensive 2D mode, ^{1}D signal can be helpful for trouble shooting purposes, and be used to for improved quantitation for the recently reported 2D assisted liquid chromatography [35]. Practically, ^{1}D detector facilitates decoupled method development on each individual dimensions without replumbing the system. Hence, ^{1}D detector is almost always included and left on during 2D-LC experiments.

On the other hand, the irradiated flow cell is actually a flow-through chamber that promotes photoreactions. With the ^{1}D detector online, the effluent of ^{1}D is essentially photo-stressed before being subjected to ^{2}D separations. Artificial peaks from photodegradation could be observed in ^{2}D, especially for photolabile compounds such as *t*-UA [36]. Fig. 7 compares two ^{2}D HILIC chromatograms of the same *t*-UA standard, acquired back to back, with and without an online ^{1}D DAD. The extra peak to the front of the *t*-UA in Fig. 7A is *cis*-urocanic acid (*c*-UA) produced in the irradiated ^{1}D DAD flow cell. The extent of such photodegradation depends on the time that analytes spend in the flow cell. With a fixed flow cell volume, the slower the ^{1}D flow rate, the longer analytes are irradiated, and therefore the greater the probability of photodegradation. Fig. 8 compares the ^{2}D HILIC chromatograms obtained using different ^{1}D flow rates. As expected, the artificial peak produced by ^{1}D DAD, *c*-UA, increased with smaller flow rates. Even at 0.2 mL/min, approximately 20% *t*-UA was isomerized due to photoexposure in the ^{1}D DAD flow cell. In comprehensive 2D experiments, where low ^{1}D flow rates are typically used to accommodate reasonable ^{2}D modulation times, the extent of photodegradation tends to be more severe. For example, Fig. 9 shows a 2D plot of a selected comprehensive SEC-HILIC 2D-LC experiment. With a ^{1}D flow rate of 15 μL/min, the *c*-UA produced in ^{1}D detector is several times more abundant than the original *t*-UA.

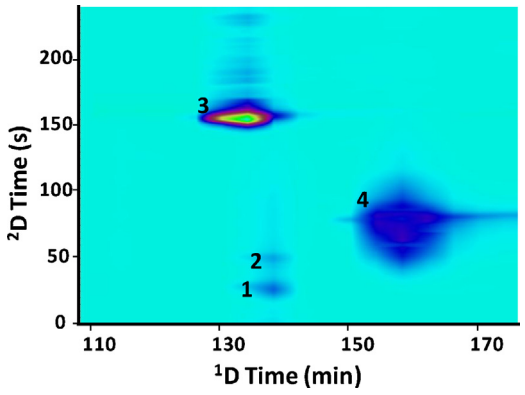

Fig. 9. Extracted ion 2D chromatograms of urocanic acid (1, *cis*; 2, *trans*), histidine (3) and sucrose (4). The ^{1}D column was 150 × 4.6 mm Waters BEH200 SEC running isocratic water/acetonitirile/formic acid 80/20/0.2 at 15 μL/min. The ^{2}D column was 150 × 4.6 mm ZIC-HILIC running 3 min gradient (90–50% organic) at 2 mL/min. The transferring loop was 80 μL at cocurrent mode with 75% fill volume (4 min modulation time). The comprehensive 2D was only conducted for selected region, where excipients were eluted from ^{1}D SEC column.

4. Conclusions

We studied histidine degradation in protein formulations using online 2D-LC by coupling SEC and HILIC separations. Successful accurate mass measurements of the degradant were achieved after separating interfering components from the sample matrix. The degradation product was identified to be *t*-UA, a histidine deamination product. In order to minimize the incompatibility of the highly aqueous SEC effluents with ^{2}D HILIC separations, smaller transferring loops, a steeper gradient and a shorter gradient time were chosen to produce symmetric peak shapes for *t*-UA in the ^{2}D.

In addition, stable-isotope dilution (SID) mass spectrometry was implemented for accurate heart-cutting 2D quantifications for the first time. The SID 2D-LC/MS method allowed transferring just the center of the ^{1}D peak for ^{2}D analysis to minimize solvent mismatch between dimensions, and in the meantime, ensured method

reproducibility despite the potential ^{1}D retention time shifts. The *t*-UA content in protein stability samples was found to increase dramatically when incubation temperature was raised from 25 to 40 °C. The *t*-UA generation was also found to be likely protein dependent, and correlated to acidic variants growth from protein degradation.

Finally, the ^{1}D DAD was found to cause photodegradation of *t*-UA to form *c*-UA. Previously, the DAD was generally considered to be non-destructive. Our experiments show that photolabile analytes could potentially degrade upon even brief irradiation in HPLC DADs. Whereas it is less of a concern in one dimensional analysis, such photodegradations in ^{1}D can be resolved in the ^{2}D chromatographic separation. Furthermore, online photodegradation cannot be minimized by reducing the exposure time of the analyte spent in ^{1}D DAD, because smaller ^{1}D flow rates are typically required in 2D-LC analysis. It is therefore necessary to bypass ^{1}D DAD when analyzing compounds that are sensitive to UV light.

Acknowledgements

The authors thank Sharon Gong for determining the isotopic distribution of labeled *trans*-urocanic acid. We would also like to thank Dr. Yongxin Zhu for reviewing the manuscript and providing helpful suggestions.

References

[1] P.J. Carter, Potent antibody therapeutics by design, Nat. Rev. Immunol. 6 (2006) 343–357.
[2] T.Y. Zhang, C. Quan, M.W. Dong, HPLC for characterization and quality control of therapeutic monoclonal antibodies, LCGC North America 32 (2014) 796–808.
[3] W. Wang, S. Singh, D.L. Zeng, K. King, S. Nema, Antibody structure, instability, and formulation, J. Pharm. Sci. 96 (2007) 1–26.
[4] B. Leader, Q.J. Baca, D.E. Golan, Protein therapeutics: a summary and pharmacological classification, Nat. Rev. Drug Discov. 7 (2008) 21–39.
[5] A. Mocsai, L. Kovacs, P. Gergely, What is the future of targeted therapy in rheumatology: biologics or small molecules, BMC Med. 12 (2014) 43–51.
[6] C.Ó. Fágáin, Understanding and increasing protein stability, Biochim. Biophys. 1252 (1995) 1–14.
[7] M.J. Akers, Excipient–drug interactions in parenteral formulations, J. Pharm. Sci. 91 (2002) 2283–2300.
[8] T.J. Kamerzell, R. Esfandiary, S.B. Joshi, C.R. Middaugh, D.B. Volkin, Protein–excipient interactions: mechanisms and biophysical characterization applied to protein formulation development, Adv. Drug Deliv. Rev. 63 (2011) 1118–1159.
[9] W.R. Wasylaschuk, P.A. Harmon, G. Wagner, A.B. Harman, A.C. Templeton, H. Xu, R.A. Reed, Evaluation of hydroperoxides in common pharmaceutical excipients, J. Pharm. Sci. 96 (2007) 106–116.
[10] J.F. Valliere-Douglass, L. Connell-Crowley, R. Jensen, P.D. Schnier, E. Trilisky, M. Leith, B.D. Follstad, J. Kerr, N. Lewis, S. Vunnum, M.J. Treuheit, A. Balland, A. Wallace, Photochemical degradation of citrate buffers leads to covalent acetonation of recombinant protein therapeutics, Prot. Sci. 19 (2010) 2152–2163.
[11] R.K. Kishore, S. Kiese, S. Fischer, A. Pappenberger, U. Grauschopf, H.C. Mahler, The degradation of polysorbates 20 and 80 and its potential impact on the stability of biotherapeutics, Pharm. Res. 28 (2011) 1194–1210.
[12] B. Mason, M. McCracken, E. Bures, B. Kerwin, Oxidation of free L-histidine by tert-butylhydroperoxide, Pharm. Res. 27 (2010) 447–456.
[13] M. Subramanian, F.N. Aleni, L. Fanget, V. Lam, E. Kaishev, Effect of histidine oxidation on the loss of potency of a humanized monoclonal antibody, AAPS PharmSci. 3 (2001) 1884.
[14] Y. Li, D. Hewitt, Y.K. Lentz, J.A. Ji, T.Y. Zhang, K. Zhang, Characterization and stability study of polysorbate 20 in therapeutic monoclonal antibody formulation by multidimensional ultrahigh-performance liquid chromatography–charged aerosol detection–mass spectrometry, Anal. Chem. 86 (2014) 5150–5157.
[15] G.J. Opiteck, J.W. Jorgenson, R.J. Anderegg, Two-dimensional SEC/RPLC coupled to mass spectrometry for the analysis of peptides, Anal. Chem. 69 (1997) 2283–2291.
[16] P. Dugo, F. Cacciola, T. Kumm, G. Dugo, L. Mondello, Comprehensive multidimensional liquid chromatography: theory and applications, J. Chromatogr. A 1184 (2008) 353–368.
[17] R.E. Majors, Multidimensional and comprehensive liquid chromatography, LCGC Asia Pacific 23 (2005) 1074–1082.
[18] R. Pascoe, J.P. Foley, A.I. Gusev, Reduction in matrix-related signal suppression effects in electrospray ionization mass spectrometry using on-line two-dimensional liquid chromatography, Anal. Chem. 73 (2001) 6014–6023.
[19] S.G. Valeja, L. Xiu, Z.R. Gregorich, H. Guner, S. Jin, Y. Ge, Three dimensional liquid chromatography coupling ion exchange chromatography/hydrophobic interaction chromatography/reverse phase chromatography for effective protein separation in top-down proteomics, Anal. Chem. 87 (2015) 5363–5371.
[20] M.R. Filgueira, Y. Huang, K. Witt, C. Castells, P.W. Carr, Improving peak capacity in fast online comprehensive two-dimensional liquid chromatography with post-first-dimension flow splitting, Anal. Chem. 83 (2011) 9531–9539.
[21] I. François, K. Sandra, P. Sandra, Comprehensive liquid chromatography: fundamental aspects and practical considerations—a review, Anal. Chim. Acta 641 (2009) 14–31.
[22] D.R. Stoll, X. Wang, P.W. Carr, Comparison of the practical resolving power of one- and two-dimensional high-performance liquid chromatography analysis of metabolomic samples, Anal. Chem. 80 (2008) 268–278.
[23] D. Lipovšek, Adnectins: engineered target-binding protein therapeutics, Protein Eng. Des. Sel. 24 (2011) 3–9.
[24] F.A. Valeev, S.M. Salikhov, O.Y. Krasnoslobodtseva, B.T. Sharipov, L.V. Spirikhin, G.A. Tolstikov, Synthesis of N-methyl urocanates of hydroxyderivatives of isocembrol, Chem. Nat. Compd. 43 (2007) 143–148.
[25] C. Wang, A. Yamniuk, J. Dai, S. Chen, P. Stetsko, N. Ditto, Y. Zhang, Investigation of a degradant in a biologics formulation buffer containing L-histidine, Pharm. Res. 32 (2015) 2625–2635.
[26] D.R. Stoll, K. O'Neill, D.C. Harmes, Effects of pH mismatch between the two dimensions of reversed-phase × reversed-phase two-dimensional separations on second dimension separation quality for ionogenic compounds—I. carboxylic acids, J. Chromatogr. A 1383 (2015) 25–34.
[27] P.G. Stevenson, D.N. Bassanese, X.A. Conlan, N.W. Barnett, Improving peak shapes with counter gradients in two-dimensional high performance liquid chromatography, J. Chromatogr. A 1337 (2014) 147–154.
[28] L. Cao, D. Yu, X. Wang, Y. Ke, Y. Jin, X. Liang, The development of an evaluation method for capture columns used in two-dimensional liquid chromatography, Anal. Chim. Acta 706 (2011) 184–190.
[29] M. Verstraeten, M. Pursch, P. Eckerle, J. Luong, G. Desmet, Thermal modulation for multidimensional liquid chromatography separations using low-thermal-mass liquid chromatography (LC), Anal. Chem. 83 (2011) 7053–7060.
[30] M. Pursch, S. Buckenmaier, Loop-based multiple heart-cutting two-dimensional liquid chromatography for target analysis in complex matrices, Anal. Chem. 87 (2015) 5310–5317.
[31] Y. Li, C. Gu, J. Gruenhagen, K. Zhang, P. Yehl, N.P. Chetwyn, C.D. Medley, A size exclusion-reversed phase two dimensional-liquid chromatography methodology for stability and small molecule related species in antibody drug conjugates, J. Chromatogr. A 1393 (2015) 81–88.
[32] D. Matějíček, Multi heart-cutting two-dimensional liquid chromatography–atmospheric pressure photoionization-tandem mass spectrometry method for the determination of endocrine disrupting compounds in water, J. Chromatogr. A 1231 (2012) 52–58.
[33] E. Yamamoto, J. Niijima, N. Asakawa, Selective determination of potential impurities in an active pharmaceutical ingredient using HPLC-SPE-HPLC, J. Pharm. Biomed. Anal. 84 (2013) 41–47.
[34] D.R. Stoll, E.S. Talus, D.C. Harmes, Evaluation of detection sensitivity in comprehensive two-dimensional liquid chromatography separations of an active pharmaceutical ingredient and its degradants, Anal. Bioanal. Chem. 407 (2015) 265–277.
[35] D.W. Cook, S.C. Rutan, D.R. Stoll, P.W. Carr, Two dimensional assisted liquid chromatography–a chemometric approach to improve accuracy and precision of quantitation in liquid chromatography using 2D separation, dual detectors, and multivariate curve resolution, Anal. Chim. Acta 859 (2015) 87–95.
[36] Y. Kurogochi, Y. Fukui, T. Nakagawa, I. Yamamoto, A note on *cis*-urocanic acid, Jpn. J. Pharmcol. 6 (1957) 147–152.